A Discrete Surface Potential Model which Accurately Reflects Channel Doping Profile and its Application to Ultra-Fast Analysis of Random Dopant Fluctuation

Hironori SAKAMOTO, Hiroshi ARIMOTO, Hiroo MASUDA, Satoshi FUNAYAMA, and Shigetaka KUMASHIRO,
MIRAI-Selete,
1120 Shimokuzawa, Sagamihara, Kanagawa 229-1198, Japan
E-mail: sakamoto.hironori@selete.co.jp

***Abstract*— A discrete surface potential model which accurately reflects channel doping profile is proposed. The proposed model is an improvement from the previously proposed model [1] in order to accurately calculate drain current in full bias region using the same mobility and velocity saturation models as TCAD. Since the proposed model is a kind of first-principal-compact-model without any unphysical fitting parameters, it can become micro-TCAD which is a by far faster and lighter substitute for conventional TCAD. As an application of the proposed model, ultra-fast calculation of threshold voltage variation induced by random dopant fluctuation using Monte-Carlo method is introduced.**

Keywords-component; Surface potential model, MOSFET, Poisson equation, channel doping profile, threshold voltage variation, random dopant fluctuation .

I. INTRODUCTION

Traditional compact models for bulk MOSFET have many fitting parameters to fulfill a stringent demand for high fitting accuracy. Moreover, the channel doping profile is quite simplified to achieve fast calculation. However, this kind of compact models cannot be used for inverse modeling of channel doping profile, process variation analysis and characteristics prediction for process condition change. Although TCAD can be used for these purposes, it takes long calculation time and the results are less accurate because of the uncertainty of the simulated impurity profiles.

Previously, we proposed a surface potential model [1] for sub-threshold characteristics calculation which accurately account for channel doping profile and is expressed by structural and process parameters only. However, it was not able to calculate drain current in the linear or saturation region. In this paper, we propose an improved model which can calculate drain current accurately in full bias region.

II. MODEL

The basic model scheme is explained. The assumed device structure and process parameters are shown in the figure 1. First, discrete nodes are generated at the channel surface from the source edge to drain edge, and channel doping profile ($N(x,z)$) for each node is set up. Next, 1-D Poisson equations of vertical direction (z-axis) for each node are solved, and then the initial surface potential (ϕ_{s0}), the effective channel concentration (N_{sub}), and the depletion depth (W_{dep}) are obtained. As for the model for 1-D Poisson equation, the previous proposed model [1] is adopted (Eq. 1).

$$C_{ox}\cdot(V_G - V_{FB} - \phi_{s0}) = C\sqrt{\frac{N_{sub}}{N_{sub0}}\cdot\Big(\beta\cdot(\phi_{s0}-V_B)-1 + \exp(-\beta\cdot(\phi_{s0}-V_B))\Big) + \exp(\beta\cdot(\phi_{s0}-2\Phi_B))} \quad \ldots(1)$$

$$C = \sqrt{\frac{2\varepsilon_{si} q\cdot N_{sub0}}{\beta}}$$

$$N_{sub} = \frac{\left(\int_0^{W_{dep}} N(x,z)dz\right)^2}{2\int_0^{W_{dep}} z\cdot N(x,z)dz}$$

$$N_{sub0} = N(x,0)$$

$$\phi_{s0} = \frac{q}{\varepsilon_{Si}}\int_0^{W_{dep}} z\cdot N(x,z)dz + V_B + \frac{1}{\beta}$$

$$\Phi_B = \frac{1}{\beta}\log\left(\frac{N_{sub0}}{n_i}\right)$$

Then, the quasi-2-D Poisson equations (Eq. 2) for each node are constructed by using them. Here, E is a term for charge reduced effect by the electric field in the channel direction (x-axis), and it is very important for accurate prediction of short channel effect (SCE) that $\Delta E(X_j)$ which is a term of charge sharing effect is properly modeled as a function of the source/drain junction depth (X_j).

$$Q_g - Q_i + E = \sqrt{C^2\frac{N_{sub}}{N_{sub0}}\cdot\Big(\beta\cdot(\phi_s - V_B)-1 + \exp(-\beta\cdot(\phi_s - V_B))\Big)} + E\cdot Q_{b0} \quad \cdots(2)$$

$$E = \varepsilon_{Si}\cdot W_{dep}\frac{d^2(\phi_s - \Phi_B)}{dx^2} + \Delta E(X_j)$$

This research was sponsored by NEDO (New Energy and Industrial Technology Development Organization, Japan)

$$Q_g = C_{ox} \cdot (V_G - V_{FB} - \phi_s)$$

$$Q_i = Q_g - \sqrt{{Q_g}^2 - C^2 \exp\left(\beta \cdot \left(\phi_s - \phi_f - 2\Phi_B\right)\right)}$$

$$Q_{b0} = C\sqrt{\frac{N_{sub}}{N_{sub0}} \cdot \left(\beta \cdot (\phi_{s0} - V_B) - 1 + \exp\left(-\beta \cdot (\phi_{s0} - V_B)\right)\right)}$$

The quasi-2-D Poisson equations and the drain current continuity equations are simultaneously solved by using Newton method. The drain current is calculated from

$$I_D = W_{gate}\mu_{eff} Q_i \frac{d\phi_f}{dx}.$$

Here, Shin's mobility model [2] and Scharfetter's velocity saturation model [3] are introduced as the default models for the effective mobility (μ_{eff}). Finally, the surface potential (ϕ_s) and quasi-Fermi potential (ϕ_f) of each node, and the drain current are obtained when Newton method is converged.

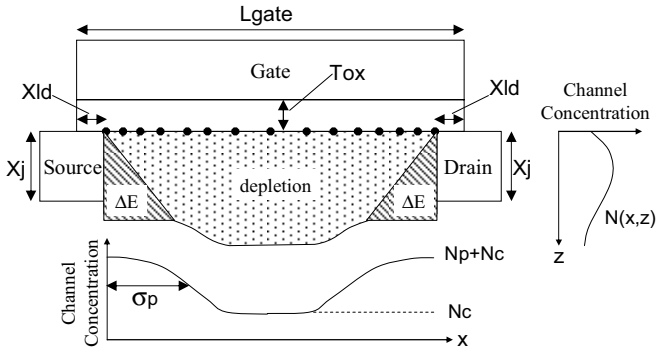

Figure 1. Device structure, process parameters, and channel doping profile of test devices. Black circles are discrete nodes.

III. RESULT

Some characteristics of test devices calculated by the proposed model are compared with TCAD simulations. The test devices correspond to low standby power (LSTP) technology of 4 process generations by ITRS [4]. The process parameters, and channel doping profiles are shown in the figure 1, and their values are shown in table I.

The threshold voltage (Vth) and saturation current (Idsat) for various gate lengths and various process generations calculated by TCAD simulations and the proposed model are shown in the figures 2 and 3. Good agreement is shown. Especially, variety of the reverse short channel effect (RSCE) is reappeared well for the different pocket/halo implantation (Fig. 4). Therefore, inverse modeling of channel doping profile based on RSCE difference is possible by using the proposed model. For comparison, the result calculated with averaged uniform concentration is shown in the figure 5. It shows clearly that channel concentration averaging is not suitable for RSCE and the drain induced barrier lowering (DIBL) reappearance.

The figures 6 and 7 show Id–Vg and Id–Vd characteristics for the test device (68.b) calculated by TCAD simulations and the proposed model. Good agreement is shown here as well.

TABLE I. VALUES OF STRUCTURAL AND PROCESS PARAMETERS OF TEST DEVICES

hp [nm]	Lmin [nm]	Tox [nm]	Vdd [V]	Ioff [pA/um]	Xj [nm]	Xld [nm]	Nc [cm^{-3}]	Np [cm^{-3}]	σp [nm]	ID
32	22	1.41	0.95	10	6.5	2	1.6E18	6.6E18	20	(32.a)
								7.2E18	15	(32.b)
								9.0E18	10	(32.c)
45	28	1.73	1.0	10	9.0	2	1.1E18	4.3E18	30	(45.a)
								4.8E18	20	(45.b)
								5.5E18	15	(45.c)
68	45	2.52	1.1	10	12.5	2	6.0E17	1.6E18	60	(68.a)
								1.75E18	40	(68.b)
								2.5E18	20	(68.c)
90	65	2.73	1.2	10	16.0	2	5.0E17	9.3E17	60	(90.a)
								1.1E18	40	(90.b)
								2.15E18	20	(90.c)

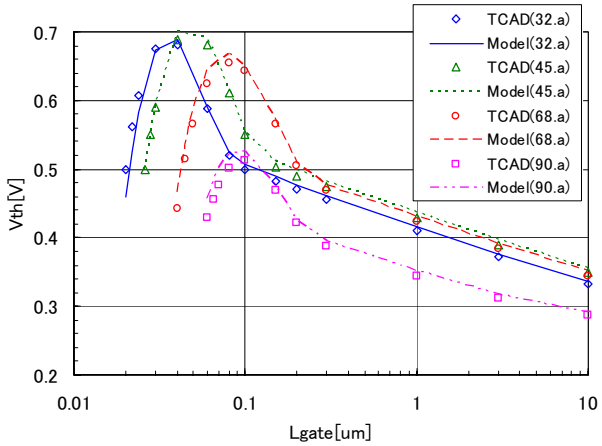

Figure 2. Vth .vs. Lgate by TCAD and our model for test devices (32.a), (45.a), (68.a), and (90.a), Vth=Vg@Id=1e-7*Lgate/Wgate, Vd=Vdd, Vb=0V.

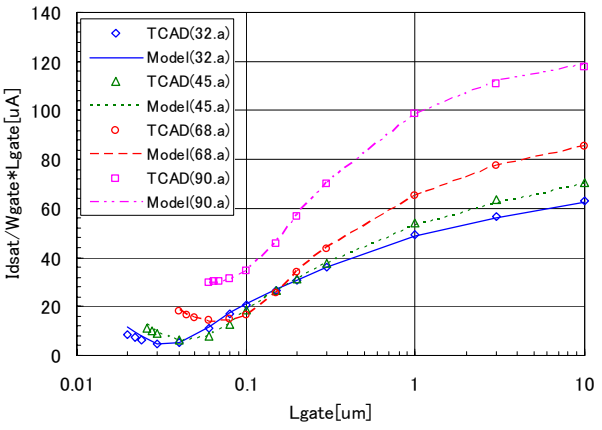

Figure 3. Idsat/Wgate*Lgate .vs. Lgate by TCAD and our model for test devices (32.a), (45.a), (68.a), and (90.a), Idsat=Id@Vd=Vg=Vdd, Vb=0V.

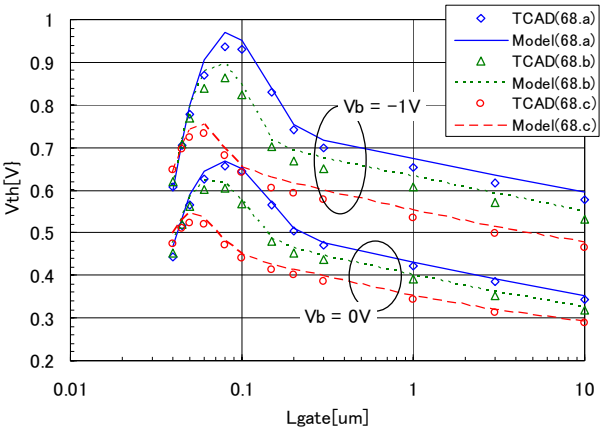

Figure 4. Vth .vs. Lgate by TCAD and our model for test devices (68.a), (68.b), and (68.c), Vd=1.1V, Vb=0V, -1V.

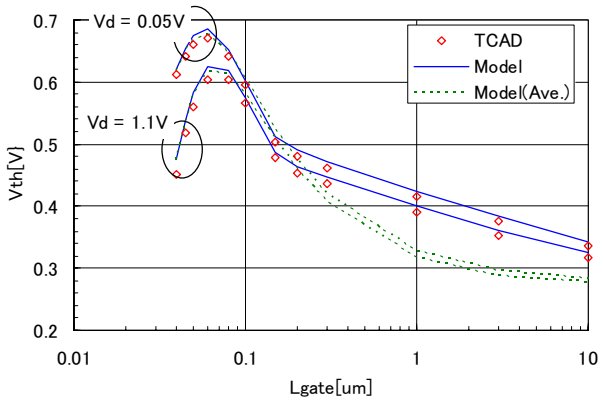

Figure 5. Vth .vs. Lgate by TCAD, our model, and our model with averaged concentration for test device (68.b), Vd=0.05V, 1.1V, Vb=0V.

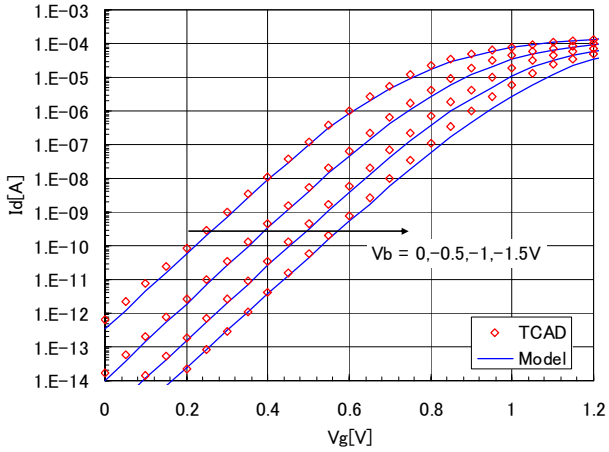

Figure 6. Id-Vg by TCAD and our model for test device (68.b), Lgate=45nm, Vd=0.05V.

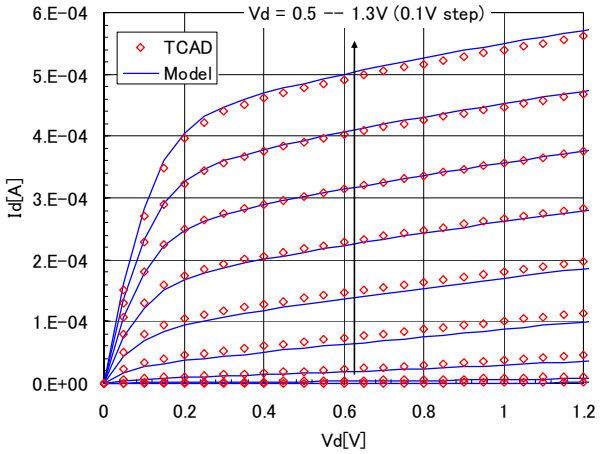

Figure 7. Id-Vd by TCAD and our model for test device (68.b), Lgate=45nm.

IV. APPLICATION

As an application of the proposed model, calculation of threshold voltage (Vth) variation induced by random dopant fluctuation using Monte-Carlo method was performed. The variance of the dopant fluctuation for each node is given by the following equation.

$$\sigma_{N_{sub}}(x) = \sqrt{\frac{4}{\Delta x \cdot W_{gate} W_{dep}^{*\,4}} \int_0^{W_{dep}} z^2 N(x,z)dz}$$

$$W_{dep}^{*} = \frac{1}{N_{sub}} \int_0^{W_{dep}} N(x,z)dz$$

This equation is driven by definition of N_{sub} which was previously proposed [1] and a weighted average of N_{sub} [5] is used. Here, Δx is a length of channel region where each node $N(x,z)$ is assigned and (x,z) is a concentration at coordinate point. For example, the variations of N_{sub} and $\phi_s - \Phi_B$ of 30 Monte-Carlo sampling points for test device (68.c) are shown in the figures 8 and 9, and the figure 10 shows the variation of Id–Vg characteristics calculated by the proposed model. Calculation time is only about 1 sec for 1,000 Monte-Carlo sampling points per bias point.

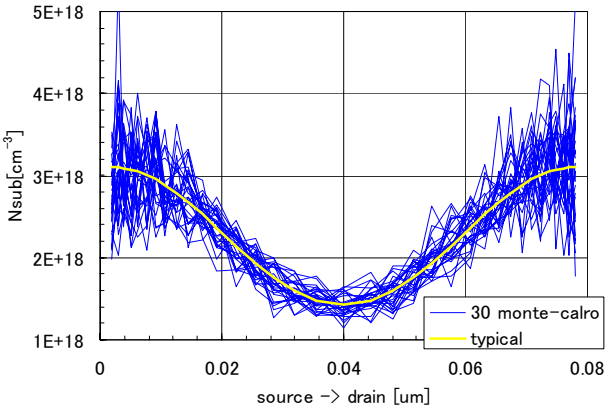

Figure 8. Variation of N_{sub} for test device (68.c), Lgate=80nm, Wgate=1um.

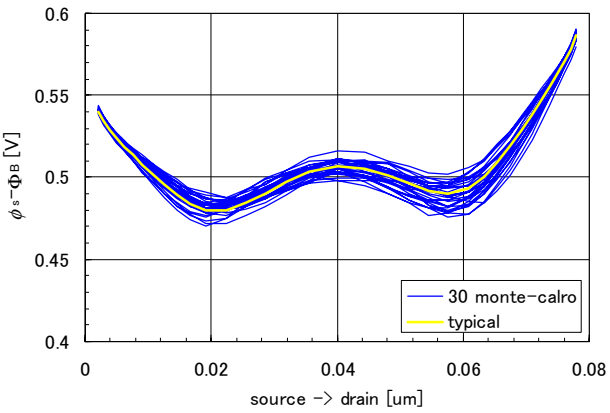

Figure 9. Variation of $\phi_s - \Phi_B$ for test device (68.c), Lgate=80nm, Wgate=1um, Vg=Vth, Vd=0.05V.

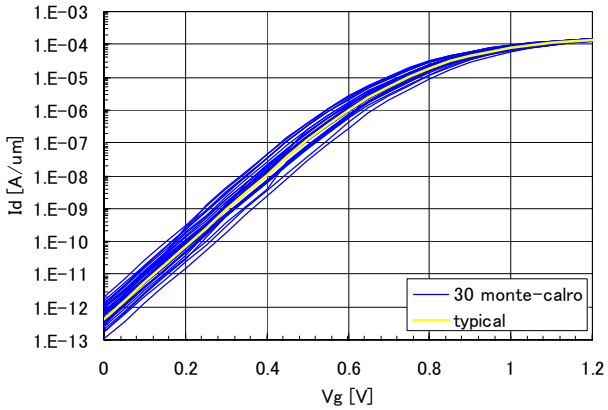

Figure 10. Variation of Id-Vg for test device (68.c), Lgate=45nm, Wgate=0.2um, Vd=0.05V.

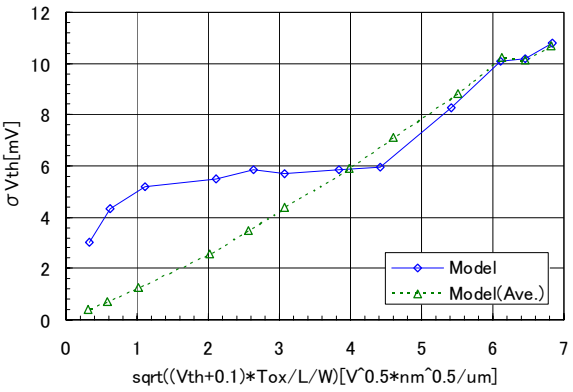

Figure 11. Takeuchi plot for test device (68.c).

Takeuchi-plot calculated is shown in the figure 11. In the case of using averaged concentration, the threshold voltage variations for long channel devices reduce with $1/\sqrt{L_{gate}W_{gate}}$ theory. But, in the case of treating concentration by pocket implantation accurately, they do not simply reduce because the threshold voltage is determined by the concentration of the pocket region.

V. CONCLUSION

The comparison with traditional compact model, TCAD, and the proposed model is summarized in table II. Since the proposed model uses only structural and process parameters and is over 1,000 to 10,000 times faster than TCAD, it can be used as a practical tool for inverse modeling of channel doping profile and calculation of electrical characteristics variation.

TABLE II. COMPARISON BETWEEN TRADITIONAL COMPACT MODEL, TCAD, AND THE PROPOSED MODEL

	Compact model	TCAD	**Proposed model**
Use fitting parameters?	Yes	No	**No**
Calculation speed (relative speed)	Very fast (>10)	Very slow (1/1,000 ~ 1/10,000)	**Fast (1)**
Applicable circuit scale	Large	Some element	**Small**
Predictability of characteristics for process condition change	Poor	Good	**Good**
Predictability of dopant induced fluctuations	Poor	Good	**Good**
Suitable for inverse modeling of channel doping profile?	No	No	**Yes**

ACKNOWLEDGMENT

This research was sponsored by NEDO (New Energy and Industrial Technology Development Organization, Japan).

REFERENCES

[1] H. Sakamoto, et al, "A Surface Potential Model for Bulk MOSFET which Accurately Reflects Channel Doping Profile Expelling Fitting Parameters", SISPAD 2008, P-38, 2008.

[2] H. Shin, et. al, "A New Approach to Verify and Derive a Transverse-Field-Dependent Mobility Model for Electrons in MOS Inversion Layers", IEEE Trans. on Electron Devices, vol.36, pp.1117-1124, 1989.

[3] D. L. Scharfetter, et. al, "Large-signal analysis of a silicon read diode oscillator", IEEE Trans. on Electron Devices, ED-16, No.1, pp.64-77, 1969.

[4] International Technology Roadmap for Semiconductors, 2007 Edition, Process Integration, Devices, and Structures, http://www.itrs.net/Links/2007ITRS/2007_Chapters/2007_PIDS.pdf

[5] K. Takeuchi, et. al, "Channel Engineering for the Reduction of Random-Dopant-Placement-Induced Threshold Voltage Fluctuation", IEDM 97, pp.841-842, 1997.